Desalination and Water Treatment
www.deswater.com

doi:10.5004/dwt.2016.1675

59 (2017) 280–286
January

Microcystin-LR degradation by hydrogen-terminated porous Si under visible light irradiation

Hangzhou Xu[a], Haiyan Pei[a, b], Hongdi Xiao[c,*], Wenrong Hu[a, b], Dezhong Cao[c]

[a]*School of Environmental Science and Engineering, Shandong University, Jinan, 250100, China, Tel./Fax +86 531 88392983, email: sdxuhangzhou@163.com (H.Z. Xu), haiyanhup@126.com (H.Y. Pei), wenrongh@sdu.edu.cn (W.R. Hu)*
[b]*Shandong provincial engineering center on Environmental Science and Technology, Jinan, 250061, China*
[c]*School of Physics, Shandong University, 250100, China. Tel. +86 531 88364329, Fax +86 531 8854886, email: hdxiao@sdu.edu.cn (H.D. Xiao), 1079763079@qq.com (D.Z. Cao)*

Received 26 November 2015; Accepted 29 June 2016

ABSTRACT

Microcystin-LR (MC-LR) produced by freshwater cyanobacteria is commonly detected in contaminated aquatic systems and their removal becomes an emerging field recently owing to the toxicity. In this paper, hydrogen-terminated porous Si (H-PSi) wafers, fabricated through a photo-electrochemical etching, were investigated as photocatalysts in MC-LR photodegradation systematically under visible light irradiation. Photoluminescence (PL) spectra and scanning electron microscope (SEM) images reveal that surface area and visible light availability of the etched samples increase with the etching times increasing, inducing that the degradation efficiency of MC-LR increases with prolonging the etching times. This degradation process can be well fitted with the pseudo-first-order kinetic model. To evaluate the optimum conditions of degradation, the relationship between the degradation efficiency of MC-LR and pH value, MC-LR concentration, or etching time is performed. We demonstrate that the maximum MC-LR degradation rate of 99% can be obtained within 2 h reaction under etching time of 10 min, initial pH of 5, and initial MC-LR concentration of 20 μg L^{-1}. In addition, it was found that H-PSi wafer exhibits a good reusability and the removal rate could be about 80% after 6 times cycle.

*Keywords***:** Photo-electrochemical etching; H-PSi wafer; Microcystin-LR; Water treatment

1. Introduction

The proliferation of cyanobacteria or blue-green algae caused by eutrophication is a serious threat to aquatic ecosystems throughout the world [1–3]. Microcystins (MCs), which are produced mainly by Microsystis aeruginosa, Anabaena spp., and Oscillatoria spp. during harmful bloom events, have a potential health risk to animals and humans who come into contact with the contaminated water [4]. Acute exposure can results in hepatic injury and in extreme cases this can prove fatal [5]. One such incident reported from Brazil resulted in the death of over 50 dialysis patients because of the use of MC-contaminated water in their treatment [5]. Furthermore, exposure to low concentrations of MCs in drinking water over a prolonged period may contribute to life threatening illnesses such as primary liver cancer [6]. To date, more than 90 types of MCs are known [7], and the most commonly detected MCs is MC-LR.

MC-LR is a cyclic heptapeptide containing the amino acid 3-amino-9-methoxy-2,6,8-trimethyl-10-phenyldeca-4,6-dienoic acid (adda), with arginine and leucine in the variable positions [8]. Moreover, MC-LR is very stable in natural waters due to its cyclic structure [9]. Unfortunately, conventional water treatment processes, such as coagulation, flocculation, sedimentation and filtration, are ineffective in removing MC-LR from drinking-water supplies [10]. Recently, chemical oxidation and microbial degradation techniques have attracted increasing interest, but there exist some new questions. Chemical oxidants such as ozone [11], and potassium permanganate [12] can completely remove

---

*Corresponding author.

1944-3994 / 1944-3986

MCs after relatively short reaction times (the half-life is about several minutes), but the low selectivity and mineralisation capacity of these chemicals can lead to the formation of degradation intermediates/byproducts [9]. Moreover, although the biodegradation of cyanotoxins cannot result in the formation of intermediates/byproducts, the half-life for the biodegradation of microcystin-LR, -LF and nodularin in water is between 4 and 18 d [13,14]. Therefore, it is necessary to develop a method for the effective removal of MC-LR from water.

Advanced oxidation processes (AOPs) have become attractive alternatives to conventional chemical oxidation methods for the generation of highly oxidizing and non-selective hydroxyl radical that display higher second-order rate constants (10^8–10^9 m^{-1} s^{-1}) than those of other oxidants [15]. Among AOPs, titanium dioxide (TiO_2) has been used as the photocatalyst widely for the photodegradation of hazardous contaminants due to its high oxidative capacity and low toxicity-features [16–19]. However, its large band gap (3.2 eV) [20] limits its applications in visible-light region, which reduces the degradation efficiency and increases the amount of the photocatalyst. Compared to TiO_2, because porous Si can produce hydroxyl radical under visible light irradiation, it has been used to photodegrade pollutants [21–23]. For example, Su et al. [21] investigated the performance of hierarchically porous silicon prepared by electro-assisted chemical etching, under visible light irradiation for the degradation of phenol. Qu et al. [22] and Wang et al. [23] fabricated the porous Si by metal-assisted chemical etching of n- and p-type Si wafers, and found that the porous Si wafer had large surface area and displayed good photodegradation of indigo carmine and methyl red. Recently, Wang et al. [23] found that porous Si with hydrogen termination in the absence of light exhibited a high degradation of methyl red due to the presence of Si-H bonds. In addition, we also fabricated the H-PSi wafer by a photo-electrochemical etching method and found that it can efficiently degrade methyl orange due to the produce lots of active radicals such as hydroxyl radical and hydrogen radical in the presence of light [24,25]. To our best knowledge, however, the degradation ability of the H-PSi wafer for hepatotoxic cyanotoxins under visible light irradiation has not carried out.

In this paper, highly ordered H-PSi wafer was prepared by a photo-electrochemical etching method under different etching times, and then the photodegradation capacity of the H-PSi wafer for MC-LR in the presence of the visible light was investigated. The main objective was two-fold, i.e., to evaluate the photodegradation effects of etching time, initial pH, and initial MC-LR concentration, and to study reusability of H-PSi wafer for MC-LR degradation.

2. Materials and methods

2.1. Chemical and reagent

MC-LR standard sample was obtained from Puhuashi Technology Development Co., Ltd (China) and kept at –25°C. A 100 mg L^{-1} standard of MC-LR solution was prepared by the addition of 1 mL of deionized water in 100 µg of solid MC-LR. NaOH, HF, and ethanol were purchased from Sinopharm Chemical Reagent Co., Ltd. (Shanghai, China). HCl was purchased from Shandong Provincial Research Institute of Chemical Industry (Jinan, China). The pH was adjusted by using NaOH (0.1 M) and HCl (0.1 M) solution. All chemicals used were of analytical grades and all solutions were prepared with deionized water (18.25 MΩ·cm).

2.2. Preparation and characteristics of H-PSi wafer

H-PSi wafers were fabricated by a photo-electrochemical etching process, which was conducted in a two-electrode cell at room temperature with p-type Si (100) wafers (1 × 1 cm^2 squares, the resistivity of 0.5–1 Ω cm, 510 µm thick) as the anode and a platinum wire as the counter electrode (cathode) in 49% HF/ethanol solution (V:V = 1:1) under room light at a constant voltage of 15 V controlled by a (GWINSTEK, GPD-3303S) source meter. After etching, the samples were rinsed with ethanol and dried in N_2. Furthermore, the etched samples with etching time of 5 min, 10 min, and 15 min were named as H-PSi-5, H-PSi-10, and H-PSi-15, respectively.

The morphologies of H-PSi wafer were characterized by a scanning electron microscope (SEM) (Zeiss, SUPRA 55) at 5 kV of electron acceleration voltage. The surface areas of H-PSi wafer with different etching times were measured by a surface area analyzer (QUADRASORB SI, Quantachrome Corporation, USA) at 77 K. The specific surface area (S_{BET}) was calculated by using the Brunauer–Emmett–Teller (BET) model. An X-ray diffraction (XRD) analysis was performed with a D 8 Advance X-ray diffractometer, to study the crystal structure of H-PSi wafer. The photoluminescence (PL) of H-PSi wafer was excited by solid state laser at 325 nm, and a wide-range optical spectrum analyzer (HORIBA Jobin Yvon iHR320) was employed to study luminescence spectra.

2.3. Photodegradation of MC-LR by H-PSi wafer

The experiments were performed in a 15 mL quartz tube, containing 3 mL MC-LR solution (initial MC-LR concentration are 20, 50, and 100 µg L^{-1}, respectively) and H-PSi wafer (1 cm^2), under constant stirring with a QB-600 High-speed Oscillation Mixer (Kylin-Bell). The reaction system was irradiated under a 30 W fluorescent lamp (TMS 018, Philips) which has a wavelength range from 390 to 760 nm [26] and a light intensity of 3000 Lux. All of the photodegradation reactions were carried out under air ambient and at 25 ± 1°C. After 30, 60, 120, and 180 min of reaction, 50 µL of the sample was taken out for the MC-LR analysis, respectively. Furthermore, the MC-LR was detected using a Beacon Microcystin ELISA kit (Beacon Analytical Systems Inc, Maine, USA). The method used for the detection of MC-LR by ELISA was performed as previously reported [27].

2.4. Kinetic analysis

The photocatalytic oxidation kinetics of many organic compounds, generally been modeled with the Langmuir-Hinshelwood equation expressed as Eq. (1),

$$r = dC/dt = kKC/(1 + KC) \tag{1}$$

Since KC is very small compared to 1.0, the presence of KC as the denominator is negligible and integrated with time t, Eq. (2) was simplified to a pseudo first order kinetic equation as below:

$$\ln(C_0/C) = kKt = k_{app}t \qquad (2)$$

where r was the reaction rate (μg L^{-1} min^{-1}), C_0 and C were the concentration of reactant at time 0 and t, respectively (mg L^{-1}), k was the reaction rate constant (min^{-1}), and K was the adsorption coefficient of targeted pollutant on the photocatalyst (L μg^{-1}). The apparent reaction rate constants (k_{app}) for the photodegradation of targeted pollutant were evaluated from experimental data using a linear regression.

3. Results and discussion

3.1. Characteristics and photodegradation activities of the H-PSi wafer

Fig. 1 shows the SEM images of H-PSi wafers prepared using different etching times: 5 min (a and d), 10 min (b and e), and 15 min (c and f). As shown in Fig. 1, pore diameter and pore depth of H-PSi wafer increase from 100 nm and 50 μm to 300 nm and 70 μm with increasing etching times, respectively. It can also be observed that the asymmetrical secondary pores exist between the first pores (see the inset of Fig. 1d–f. Similar structures have been observed in previous reports [25,28]. These results indicate that the surface-to-volume (S/V) ratio of etched samples increases with increasing the etching times, which is in good agreement with the BET specific surface area (see Table 1).

To investigate the quality of etched Si wafers, the structural and optical properties were analyzed. The XRD patterns of H-PSi wafers obtained using different etching times are shown in Fig. 2. The intensity of H-PSi (400) peaks increases with increasing the etching time,

Table 1
Characteristics of H-PSi wafers at different etching times

Etching time (min)	Pore diameter (nm)	Pore depth (μm)	Pore density (pores/cm^2)	Porosity (%)	Specific surface area (m^2 g^{-1})
5	100	50	1.6 × 108	1.6	3.95
10	300	65	2.4 × 108	21.6	25.43
15	300	70	2.5 b × 108	22.5	27.32

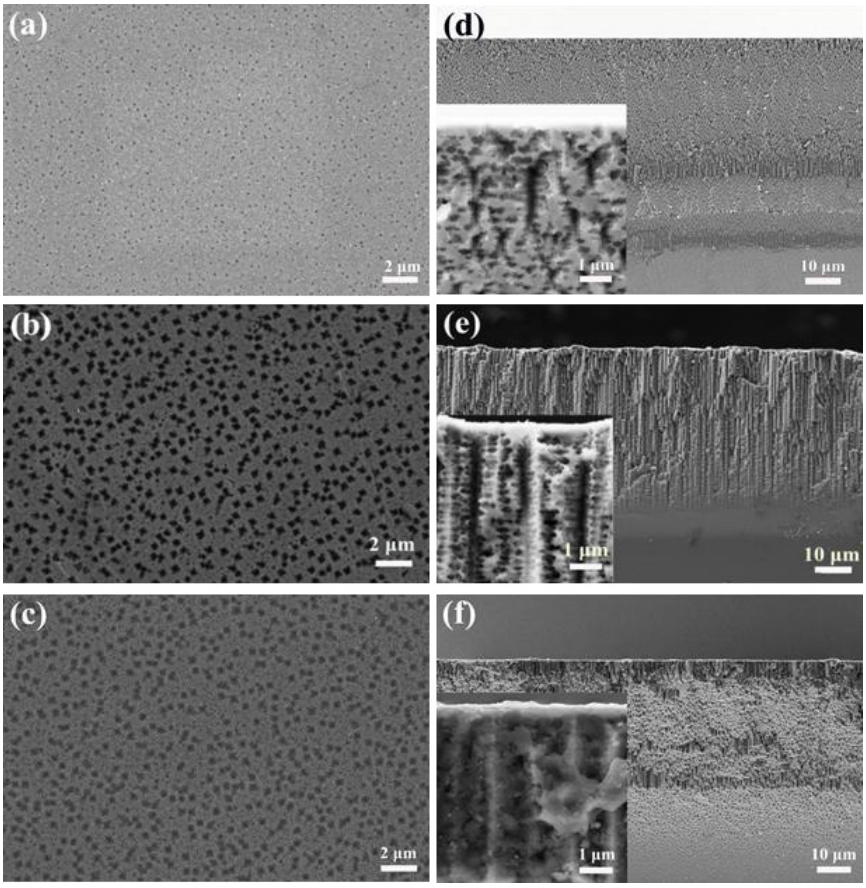

Fig. 1. The top-view and cross-sectional SEM images of H-PSi wafer obtained under the etching times: (a and d) 5 min, (b and e) 10 min, and (c and f) 15 min for 15 V. Insets are the corresponding magnified cross section images.

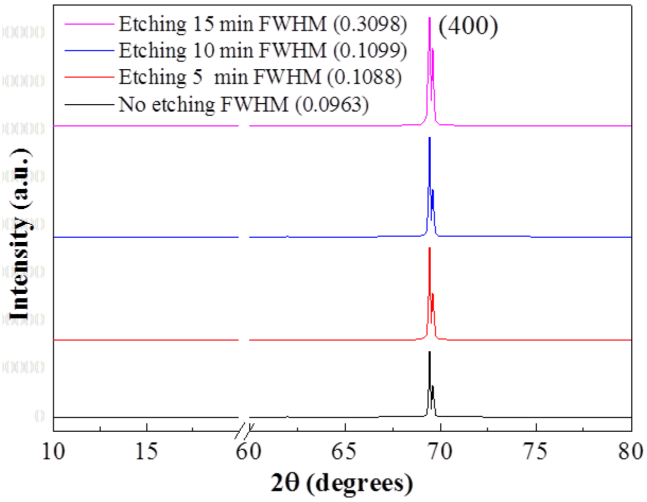

Fig. 2. X-ray diffraction pattern of H-PSi wafer etched at different etching times at room temperature. Etching voltage: 15 V.

which is, at least partially, due to physical surface roughening which means that diffraction is out-coupled from the crystal more efficiently, whereas the full width at half maximum (FWHM) of the XRD peaks of the etched Si wafers presents a slight widening with the etching time increasing, indicating that the etching can lead to the increase of defect density [29]. Fig. 3 shows the PL spectra for H-PSi wafers in the range of 500–900 nm. It was found that prolonging etching time results in an increase of PL intensity as well as a blue shift from ~1.8 eV to ~1.89 eV, which may be due to the increasing of porous porosity (see Table 1) and quantum confinement effect of nanocrystalline particles [25].

To evaluate the effect of etching time on the photodegradation of MC-LR under visible light irradiation, the relationship between the etching time and photodegradation of MC-LR by H-PSi wafer was investigated. As shown in Fig. 4a, the amount of MC-LR degraded by H-PSi wafer increased from 41.6 to 97.4% after 180 min of reaction with increasing the etching time from 5 to 15 min. The pseudo first-order kinetics for MC-LR degradation by H-PSi wafer is given in Fig. 4b. The values of R^2 for flat Si, H-PSi-5, H-PSi-10, and H-PSi-15 were 0.9718, 0.9842, 0.9922, and 0.9976, respectively, confirming the first order trend of the degradation of MC-LR by H-PSi wafer. The k_{app} values of flat Si, H-PSi-5, H-PSi-10, and H-PSi-15 were calculated as 0.0003, 0.0033, 0.0173, and 0.0196 min^{-1}, respectively. The results suggested that the apparent reaction rate constant for H-PSi wafer increased with higher S/V ratio. Meanwhile, it was also found that the k_{app} value of H-PSi-10 was similar to H-PSi-15, which may be attributed to the similar porosity (see Table 1).

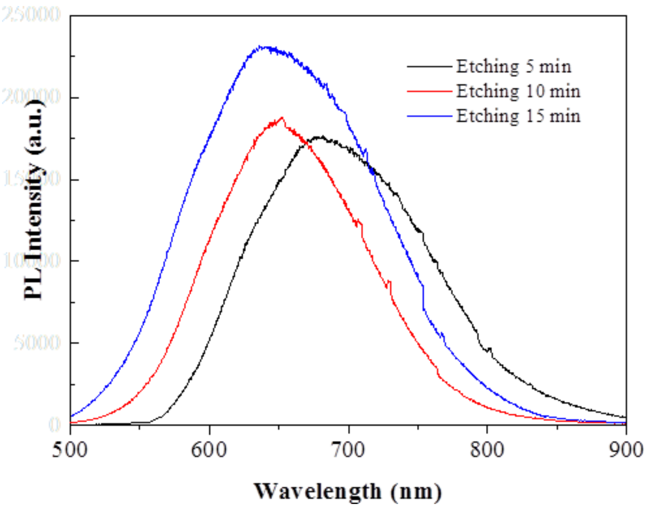

Fig. 3. Photoluminescence spectra of H-PSi wafer etched at different etching times at room temperature. Etching voltage: 15 V.

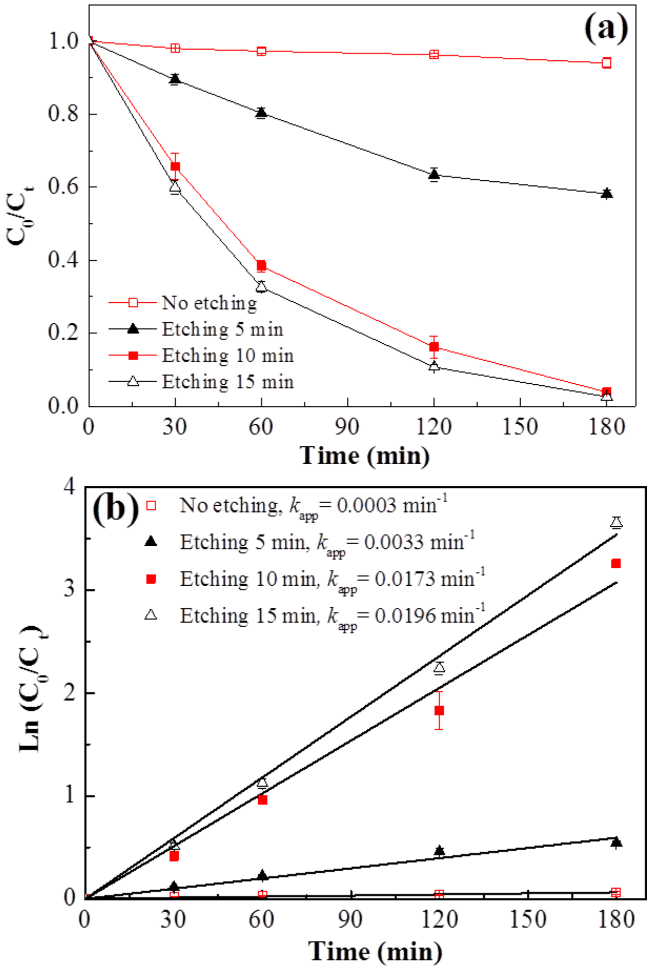

Fig. 4. Degradation of MC-LR by H-PSi wafer with different etching times under visible light irradiation (a) and the pseudo-first-order kinetics for photodegradation of MC-LR (b). Etching voltage: 15 V. Initial pH: 7. Initial MC-LR concentration: 50 μg L^{-1}.

3.2. Photodegradation of MC-LR by H-PSi wafer

The impact of the experimental variables (initial pH and initial MC-LR concentration) on the degradation of MC-LR by H-PSi wafer was evaluated using a factorial design system. Each variable was studied at two values (initial pH levels of 5 and 9 and initial MC-LR concentrations of 20 and 100 μg L^{-1}), which created a 2^2 complete factorial design around a central point (initial pH: 7, initial MC-LR concentration: 50 μg L^{-1}) (Table 2). Furthermore, H-PSi wafer was chosen with the etching time of 10 min according to previous results (Fig. 4), and the analytical response corresponds to the MC-LR degradation (%) at a 120 min reaction time.

To investigate the influence of initial pH and MC-LR concentration, and their interaction on MC-LR degradation by H-PSi wafer, the geometric representation of 22 factorial design was designed (Fig. 5). The central point was assayed in triplicate, showing a mean standard deviation (SD) of 1.9%, and it can be found that the pH has a significantly negative effect (–36.5, which was calculated by [(67 + 52)–(93 + 99)]/2 = –36.5) on the degradation capacity of H-PSi wafer. The strong dependence of photodegradation ability on pH presumably results from the following two reasons. On the one hand, Si-H bonds are presented on the surface of H-PSi wafer, therefore, the vibration by the high-speed shock tester breaks Si–H bonds can lead to the formation of Si dangling bonds with activated $\cdot Si^+$ and $\cdot H^-$ radicals. These free negatively charged hydrogen radicals may recombine with hydrogen ion in water via reactions $\cdot H^- + H^+ \rightarrow 2\cdot H$ [25,30], promoting the production of hydrogen radicals aforementioned. On the other hand, the hydrophobicity of MC-LR increases as pH decreases. Through the hydrophobic effect, hydrophobic compounds (MC-LR) preferentially moved to H-PSi wafer surface from the bulk of aqueous solvents [17,31]. Hence, the degradation rate of MC-LR by H-PSi wafer could be improved significantly with low pH value.

Table 2
Factorial design 22 matrix for the study of MC-LR degradation under the photodegradation processes.Etching voltage: 15 V. Etching time: 10 min. Reaction time: 120 min

Variable	Level (–)	Level (0)	Level (+)
pH	5	7	9
MC-LR (μg L^{-1})	20	50	100
Experiment	Variable		MC-LR degradation (%)
	pH	MC-LR	
1	–		99 ± 0.9
2	–	+	93 ± 1.5
3	+	–	67 ± 2.1
4	+	+	52 ± 1.1
5	0	0	88 ± 1.9

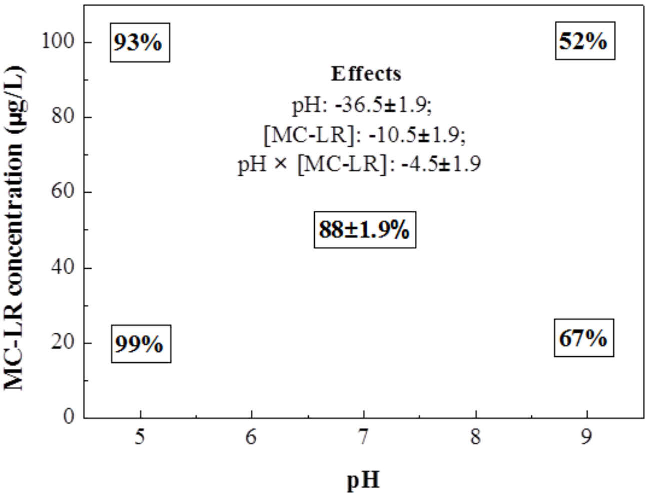

Fig. 5. A geometric representation of the 2^2 factorial design used to evaluate the effects of initial pH and initial MC-LR concentration on the degradation efficiency of the photodegradation processes. Etching voltage: 15 V. Etching time: 10 min. Reaction time: 120 min. The numbers in the boxes represent the degradation (%) of MC-LR at a reaction time of 120 min.

The initial MC-LR concentration also has a negative effect (–10.5, which was calculated by [(93 + 52)–(99 + 67)] = –10.5) on the degradation efficiency of H-PSi wafer. The yield rate of free radicals was remained as a constant with the same H-PSi wafer area, hence, the increasing concentration of MC-LR resulted in a decrease in the ratio of decomposed amount of MC-LR to the total amount of MC-LR [31], presumably resulting from that more active sites are covered by MC-LR molecules and intermediates generated by photodegradation of MC-LR, which reduce the production of hydroxyl radicals on the surface of the H-PSi wafer and cause a deactivation of active sites of the catalyst, resulting in the degradation efficiency decrease [32]. Furthermore, the interaction of initial pH and initial MC-LR concentration also has a slightly negative effect (–4.5, which was calculated by [(52 + 99)–(93 + 67)] = –4.5) on the degradation efficiency of H-PSi wafer. This result means that the increase of initial pH and MC-LR concentration at the same time will lead to a lower degradation efficiency of H-PSi wafer than the individual increase of initial pH and MC-LR concentration.

3.3. *Reusability of H-PSi wafer for MC-LR degradation*

The reusability of the H-PSi wafer was investigated by repeating the photodegradation of MC-LR under visible light irradiation for 120 min six times. Because of the formation of oxide layers on the Si surface or inside the pores, the degradation rate decreases obviously with increasing the recycle times [23]. Hence, after each cycle, the H-PSi wafer was taken out and put into the HF solution (5%) for 1 min, which can remove the oxide layers formed during the photodegradation of MC-LR and recover the photodegradation activity of H-PSi wafer [23], then washed thoroughly with DI water before new experiments. Compared Fig. 6a, b with Fig. 1b, e, it is obvious that the surface of H-PSi wafer has some damage, which might be attributed to the HF to remove the oxide layers on the surface of porous Si wafer after each cycle. Furthermore, the XRD pattern of the H-PSi wafer after 6 times cycle was detected and the result is shown in Fig. 7. Because the damage of H-PSi wafer surface, the intensity of H-PSi (400) peak and FWHM increased compare with that before recycle. However, it is encouraging to find that after six repeated experiments, the photodegradation efficiencies were remarkably stable, and during the last run was still around 80% (Fig. 8). The H-PSi wafer therefore possesses remarkable stability.

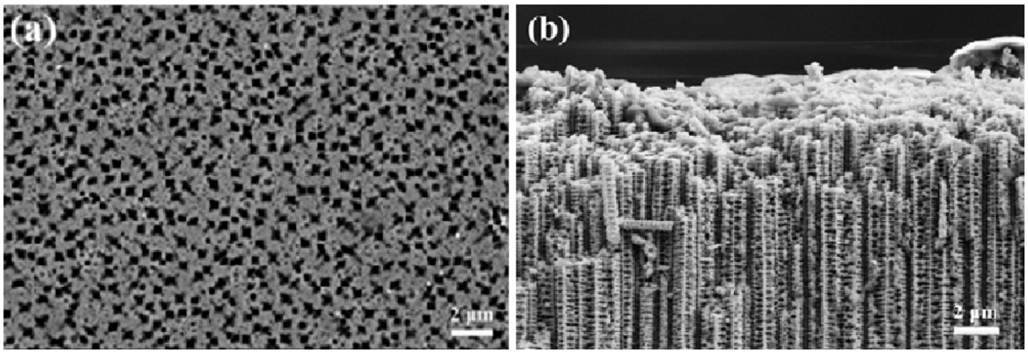

Fig. 6. The top-view and cross-sectional SEM images of H-PSi wafer reused for 6 times. Etching voltage: 15 V. Etching time: 10 min.

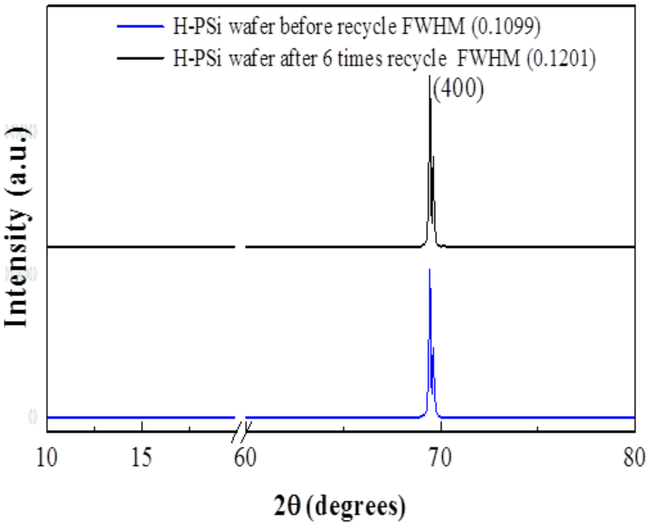

Fig. 7. Photoluminescence spectra of H-PSi wafer before recycle and after 6 times recycle at room temperature. Etching voltage: 15 V. Etching time: 10 min.

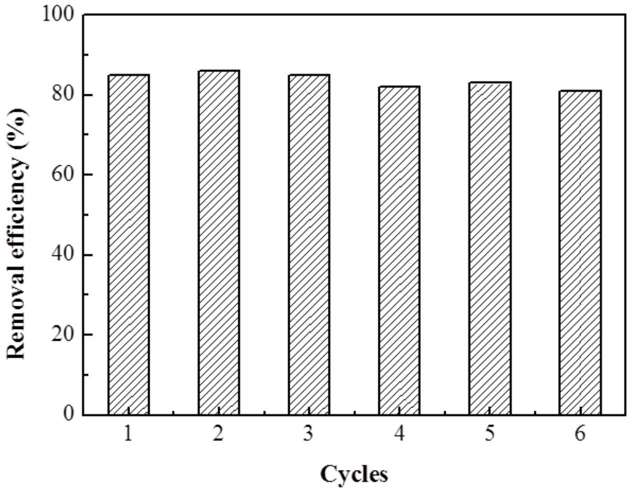

Fig. 8. Degradation efficiencies of MC-LR by H-PSi wafer for 6 experimental runs. Etching voltage: 15 V. Etching time: 10 min. Reaction time: 120 min. Initial pH: 7. Initial MC-LR concentration: 50 μg L^{-1}.

4. Conclusions

The H-PSi wafer was fabricated by a photo-electrochemical etching and characterized with XRD, SEM, and PL, and then it was used to remove MC-LR from aqueous solution under visible light irradiation. The degradation efficiency of MC-LR was influenced by several parameters which includes etching time of the H-PSi wafer, initial pH, and initial MC-LR concentration. When the etching time is 10 min, initial pH is 5, and initial MC-LR concentration is 20 μg L^{-1}, MC-LR degradation efficiency could be 99% within 2 h reaction. Furthermore, the H-PSi wafer exhibits a good reusability. Hence, H-PSi wafer is a highly efficient photocatalyst for MC-LR degradation in aqueous solutions. This study provides a promising technique to remove the toxic effectively and prevent the harm of MC-LR to drinking water production.

Acknowledgements

This work was supported by the International Science & Technology Cooperation Program of China (2010DFA91150), International Cooperation Research of Shandong Province (2011176), Science and Technology Development Project of Shandong Province (2012GHZ30020), National Science Fund for Excellent Young Scholars (51322811), National Natural Science Foundation of China (61376069), Natural Science Foundation of China (51478251), The Program for New Century Excellent Talents in University of the Ministry of Education of China (Grant No. NCET-12-0341).

References

[1] P.B.O. Ochumba, D.I. KibaaraI, Observations on blue-green algal blooms in the open waters of Lake Victoria, Kenya, Afr. J. Ecol., 27 (1989) 23–34.
[2] D.W. Schindler, R.E. Hecky, G.K. McCullough, The rapid eutrophication of Lake Winnipeg: Greening under global change, J. Great Lakes Res., 38 (2012) 6–13.
[3] M. Yang, J.W. Yu, Z.L. Li, Z.H. Guo, M. Burch, T.F. Lin, Taihu Lake not to blame for Wuxi's woes, Science, 319 (2008) 158.
[4] D.D. Yin, N.Y. Gao, K.J. Zhang, L. Li, Y. Deng, Microcystin-RR degradation by ozonation, Desal. Water Treat., 55 (2015) 1060–1067.
[5] J. Dunn, Algae kills dialysis patients in Brazil, Brit. Med. J., 312 (1996) 1183–1184.
[6] I. Liu, L.A. Lawton, D.W. Bahnemann, L. Liu, B. Proft, P.K.J. Robertson, The photocatalytic decomposition of microcys-

tin-LR using selected titanium dioxide materials, Chemosphere, 76 (2009) 549–553.

[7] M. Ziegmann, M. Abert, M. Muller, F.H. Frimmel, Use of fluorescence fingerprints for the estimation of bloom formation and toxin production of Microcystis aeruginosa, Water Res., 44 (2010) 195–204.

[8] G.F. Dai, C.Y. Quan, X.Z. Zhang, J. Liu, L.R. Song, Fast removal of cyanobacterial toxin microcystin-LR by a low-cytotoxic microgel-Fe(III) complex, Water Res., 46 (2012) 1482–1489.

[9] L.C. Jacobs, P. Peralta-Zamora, F.R. Campos, R. Pontarolo, Photocatalytic degradation of microcystin-LR in aqueous solutions, Chemosphere, 90 (2013) 1552–1557.

[10] A.M. Keijola, K. Himberg, A.L. Esala, K. Sivonen, L. Hiisvirta, Removal of cyanobacterial toxins in water treatment processes: laboratory and pilot-scale experiments, Toxic. Assess., 3 (1988) 643–656.

[11] S. Brooke, G. Newcombe, B. Nicholson, G. Klass, Decrease in toxicity of microcystins LA and LR in drinking water by ozonation, Toxicon, 48 (2006) 1054–1059.

[12] E. Rodriguez, M.E. Majado, J. Meriluoto, J.L. Acero, Oxidation of microcystins by permanganate: reaction kinetics and implications for water treatment, Water Res., 41 (2007) 102–110.

[13] C. Edwards, D. Graham, N. Fowler, L.A. Lawton, Biodegradation of microcystins and nodularin in freshwaters, Chemosphere, 73 (2008) 1315–1321.

[14] A. Torunska, J. Bolalek, M. Plinski, H. Mazur-Marzec, Biodegradation and sorption of nodularin (NOD) in fine-grained sediments, Chemosphere, 70 (2008) 2039–2046.

[15] M. Mohajerani, M. Mehrvar, F. Ein-Mozaffari, An overview of the integration of advanced oxidation technologies and other processes for water and wastewater treatment, Int. J. Eng., 3 (2009) 120–146.

[16] M.G. Antoniou, J.A. Shoemaker, A.A. de la Cruz, D.D. Dionysiou, LC/MS/MS structure elucidation of reaction intermediates formed during the TiO_2 photocatalysis of microcystin-LR, Toxicon, 51 (2008) 1103–1118.

[17] L.A. Lawton, P. Robertson, B. Cornish, I.L. Marr, M. Jaspars, Processes influencing surface interaction and photocatalytic destruction of microcystins on titanium dioxide photocatalysts, J. Catal., 213 (2003) 109–113.

[18] P.K.J. Robertson, L.A. Lawton, B. Munch, J. Rouzade, Destruction of cyanobacterial toxins by semiconductor photocatalysis, Chem. Commun., 4 (1997) 393–394.

[19] T. Fotiou, T.M. Triantis, T. Kaloudis, L.M. Pastrana-Martínez, V. Likodimos, P. Falaras, A.M.T. Silva, A. Hiskia, Photocatalytic degradation of microcystin-LR and off-odor compounds in water under UV-A and solar light with a nanostructured photocatalyst based on reduced graphene oxide-TiO_2 composite. Identification of intermediate products, Ind. Eng. Chem. Res., 52 (2013) 13991–14000.

[20] D. Pjević, T. Marinkovic, J. Savić, N. Bundaleski, M. Obradović, M. Milosavljević, M. Kulik, Influence of substrate temperature and annealing on structural and optical properties of TiO_2 films deposited by reactive e-beam evaporation, Thin Solid Films, 591 (2015) 224–229.

[21] J.Y. Su, H.T. Yu, X. Quan, S. Chen, H. Wang, Hierarchically porous silicon with significantly improved photocatalytic oxidation capability for phenol degradation, Appl. Catal. B Environ., 138–139 (2013) 427–433.

[22] Y.Q. Qu, X. Zhong, Y.J. Li, L. Liao, Y. Huang, X.F. Duan, Photocatalytic properties of porous silicon nanowires, J. Mater. Chem., 20 (2010) 3590–3594.

[23] F.Y. Wang, Q.D. Yang, G. Xu, N.Y. Lei, Y.K. Tsang, N.B. Won, J.C. Ho, Highly active and enhanced photocatalytic silicon nanowire arrays, Nanoscale, 3 (2011) 3269–3276.

[24] H.Z. Xu, H.D. Xiao, H.Y. Pei, J.S. Cui, W.R. Hu, Photodegradation activity and stability of porous silicon wafers with (100 and (111) oriented crystal planes, Micropor. Mesopor. Mater., 204 (2015) 251–256.

[25] H.Z. Xu, H.Y. Pei, H.D. Xiao, W.R. Hu, Degradation mechanism of hydrogen-terminated porous silicon in the presence and in the absence of light, AIP Adv., 5 (2015) 67–125.

[26] N. Naderi, M. Hashim, Effect of surface morphology on electrical properties of electrochemically-etched porous silicon photodetectors, Int. J. Electrochem. Sci., 7 (2012) 11512–11518.

[27] F. Sun, H.Y. Pei, W.R. Hu, X.Q. Li, C.X. Ma, R.T. Pei, The cell damage of *Microcystis aeruginosa* in PACl coagulation and floc storage processes, Sep. Purif. Technol., 115 (2013) 123–128.

[28] N. Naderi, M. Hashim, Effect of surface morphology on electrical properties of electrochemically-etched porous silicon photodetectors, Int. J. Electrochem. Sci., 7 (2012) 11512–11518.

[29] M. Jayachandran, M. Paramasivam, K.R. Murali, D.C. Trivedi, M. Raghavan, Synthesis of porous silicon nanostructures for photoluminescent devices, Mater. Phys. Mech., 4 (2001) 143–147.

[30] Z.H. Chen, Y.B. Tang, Y. Liu, Z.H. Kang, X.J. Zhang, X. Fan, C.S. Lee, I. Bello, W.J. Zhang, S.T. Lee, Dye degradation induced by hydrogen-terminated silicon nanowires under ultrasonic agitations, J. Appl. Phys., 105 (2009) 34–307.

[31] X. Sui, X.R. Wang, H.H. Huang, G.T. Peng, S.B. Wang, Z.Q. Fan, A novel photocatalytic material for removing microcystin-LR under visible light irradiation: degradation characteristics and mechanisms, PLoS one, 9 (2014) e95798.

[32] Y.L. Su, Y.R. Deng, L. Zhao, Y.X. Du, Photocatalytic degradation of microcystin-LR using TiO_2 nanotubes under irradiation with UV and natural sunlight, Chinese Sci. Bull., 58 (2013) 1156–1161.